FACTA UNIVERSITATIS
Series: **Mechanical Engineering** Vol. 20, Nº 1, 2022, pp. 167 - 176
https://doi.org/10.22190/FUME201004026R

Original scientific paper

DESIGN AND CALIBRATION OF THE SYSTEM SUPERVISING BELT TENSION AND WEAR IN AN INDUSTRIAL FEEDER

Tomasz Ryba, Miroslaw Rucki, Zbigniew Siemiatkowski, Damian Bzinkowski, Michal Solecki

Kazimierz Pulaski University of Technology and Humanities in Radom, Poland

Abstract. *In the paper, the issue of the supervision of belt tension and wear in industrial feeder is addressed. The designed system is based on strain gauges that are built into the roller and are subject to the belt pressure at each revolution. In order to assess the effectiveness of this system, calibration and uncertainty analysis was performed. As a result, it was demonstrated that the main source of uncertainty was the function of approximation, while the others were orders of magnitude smaller. The final function provided results with accuracy of ca. 10% of actually measured value, which was assumed to be a good result for this particular industrial application.*

Key Words: *Industrial Feeder, Belt, Wear, Measurement, Calibration*

1. INTRODUCTION

In the context of smart factories and "Industry 4.0," preventive maintenance based on the concept of flexible and diverse maintenance levels is widely introduced [1, 2]. It is highly desirable to perform condition-based maintenance capable of identifying fault monitoring actual condition of the system obtained from in-situation, no-invasive tests and measurements [3]. The inspection workload for preventive maintenance of a large-scale distribution facility is enormous because it encompasses a large amount of equipment such as conveyors and sorters [4]. Implementation of the cyber-physical systems for performance monitoring in production intralogistics requires reliable data about actual state of the conveyors and their elements [5].

However, in the area of industrial belt feeders, no such a system for in-situ tension monitoring was proposed so far. Extensive theoretical background for work conditions and calculations of the belt feeders can be found in the literature [6] including 3D models of the tensions [7]. Analysis of various internal structures and the type of the material falling onto

Received October 04, 2020 / Accepted February 18, 2021
Corresponding author: Miroslaw Rucki
Faculty of Mechanical Engineering, Kazimierz Pulaski University of Technology and Humanities in Radom, Krasickiego Str. 54, 26-600 Radom, Poland
E-mail: m.rucki@uthrad.pl

a conveyor belt and effects thereof on the incurred damage enabled the damage classification [8]. It was demonstrated that the operating characteristics could be predicted based on experimental measurements, with a specific example focusing on the prediction of the contact force – tension force relationship [9]. There are also propositions concerning diagnostics during exploitation, such as a non-invasive system able to monitor the joints of the monitored belt in order to detect critical elongation [10]. Another project involved steel ropes inside the belt material, so that the magnetic field could be measured directly on the feeder [11]. Some other solutions propose the belts with built-in tensors, but after the belt is damaged or worn out, the entire tensor system is lost with no possibility of further use.

Recently, the test equipment for real time belts tension detection during the conveyor work was proposed [12] and patented [13]. It was necessary, however, to prove its capability to detect tension releases caused by wear and damages of the belt. For that purpose, the calibration procedure was performed using a special intermediate device described below.

2. Device Concept and Calibration Issue

The essence of the novel measurement system supervising belt tension and wear is presented in Fig. 1. Application of strain gauges directly on the roller made it possible to obtain data concerning the belt conditions during its work. Transducers are placed inside the empty roll subjected to the load-dependent on the belt tension.

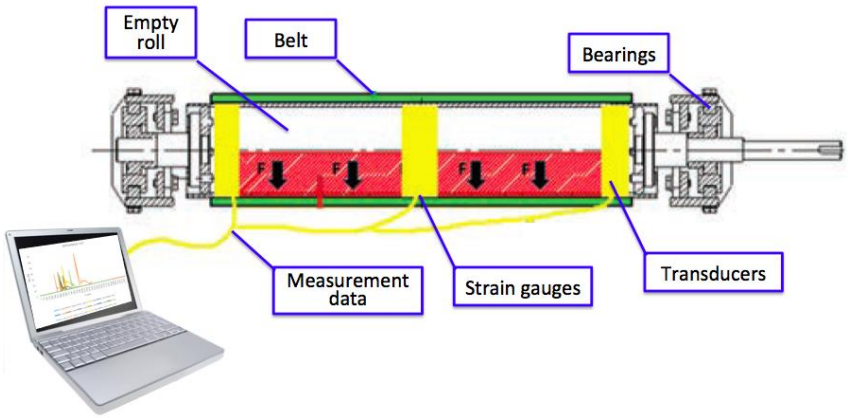

Fig. 1 Scheme of the measurement system

The strain gauges of the type CP 152 NS (ø16) were chosen because of low costs, availability in the market, flexibility in the applications, good dynamic characteristics, and a large enough measuring range. Their nominal operating voltage was 1.5 [V] in the temperature range from -40 up to 80 [°C]. Initial tests provided promising results since the strain gauges placed along the roller gave the measurement results according to the actual pressure distribution. Namely, when the belt was under asymmetrical load, one gauge shows higher tension, while the other detected slight release. It is shown in Fig. 2, view from the top, with the load placed closer to gauge t_2, but in the actual scale this slight force decrease is not clearly distinguishable.

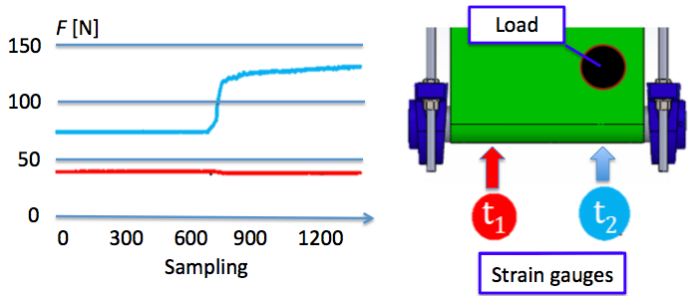

Fig. 2 Load registered by two gauges

Conditions of the belt tension monitoring through measurement of its pressure on the roller are dynamic. As a result, registered pressure reveals an undesirable peak in the very first moment of contact between the belt and the strain gauge, as shown in Fig. 3.

Even though this peak is quite repeatable, it makes difficult to perform the correct analysis of the obtained measurement signal. The nominal strength of belt K_n is calculated from the following equation [6]:

$$K_n = \frac{Sr_{max}}{1000 \cdot B} \cdot k_e \cdot k_b \tag{1}$$

where Sr_{max} is the maximal force in the belt during startup [N], B is belt width [m], k_e is exploitation safety factor, and k_b is the factor of tension concentration in joints. Hence, the maximal pressure registered with the measurement system should not be a result of gauge excitation.

Having noticed this feature generated by the dynamic mechanical contact between the belt and the strain gauge, it was decided to modify the fixation of the gauge. It was found necessary to perform calibration of the strain gauge as part of the system, as it works in real conditions. After modification, however, another issue emerged, namely, of how to ensure steady distribution of the pressure on the calibrated strain gauge surface, with stable and repeatable fixation.

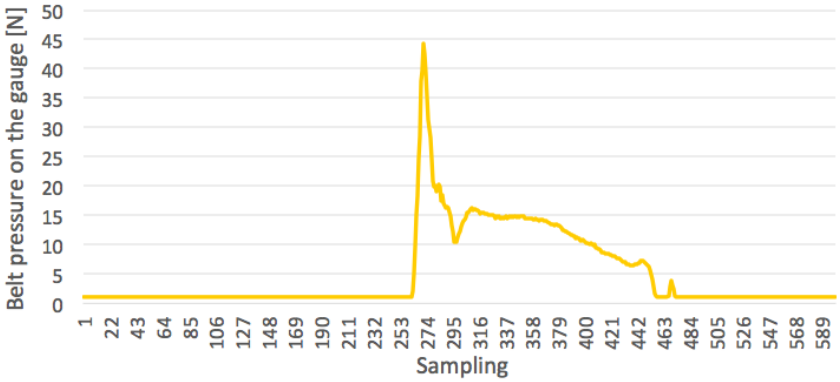

Fig. 3 Signal from the strain gauge obtained during rotation of the roller

3. Calibration Apparatus and Conditions

To perform the calibration procedure correctly, novel instrumentation was designed. Its aim was to ensure a repeatable contact area between the reference mass standard and the strain gauge surface. Stable vertical movement transmitting the mass on the gauge surface was achieved through two precise shafts ø10 fixed in the lower body, with linear bearings denoted LM10UU. Fig. 4a presents the designed calibration apparatus and 4b the intersection of its main part. The numbers denote as follows: 1 – calibrated strain gauge, 2 – upper body of calibration instrumentation, 3 – reference mass standard, 4 – shaft with rounded upper end, 5 – round nut, 6 – bolt M5×20, 7 – upper body. Upper surface of body 7 was shaped in a special way, enabling steady distribution of the reference weight during calibration.

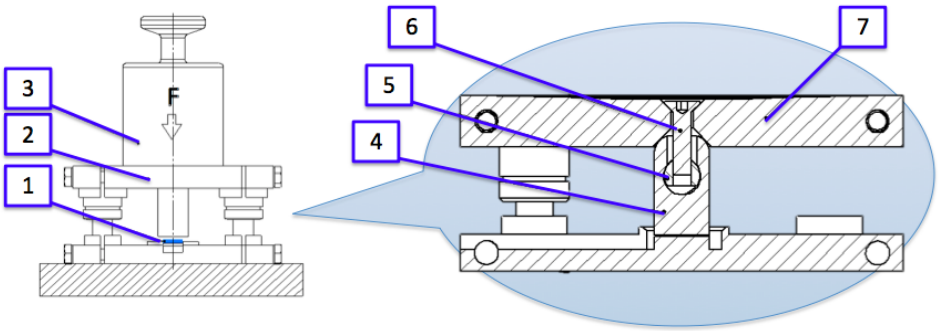

Fig. 4 Concept of the calibration instrumentation (description in the text)

To project and produce the instrumentation, SolidWorks software was used. The models were exported to *.stl files in order to apply additive manufacturing (AM) technology. AM is a very useful technology for fabricating complex shape details out of polymers [14] and even for very strong elements [15]. A method known as FDM (*Fused Deposition Modeling*) was applied, where molten fibers are extruded and deposited to print stacks of 2D cross-sections and finally form complex 3D products [16]. 3D printer type 4MAX was used, with working space 220×220×300 [mm] (width × length × height). The material was PLA fiber of diameter 1.75 [mm], deposition was performed at temperature 225 [°C], grid method, printing speed 50 [m/s]. Fig. 5, left, presents the SolidWorks model, and Fig. 5, right, photo of printed and assembled instrumentation.

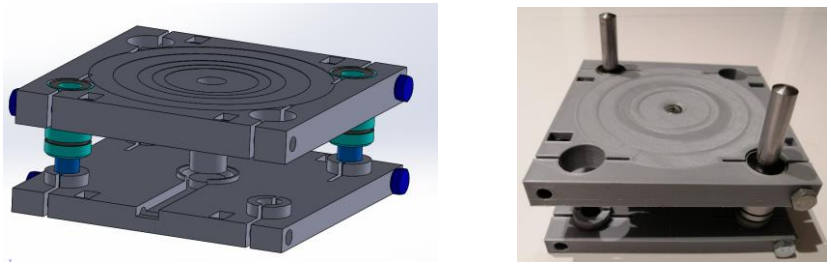

Fig. 5 Calibration instrumentation model and its realization

The calibration procedure was performed in the laboratory of the Radwag Company in Radom, Poland. Its uncertainty is affected mainly by the following factors:

- uncertainty of weights,
- uncertainty of reading resolution and approximation error,
- uncertainty of environmental conditions.

Thus, mass indication m_i of the strain gauge and its uncertainty can be expressed with the equation as follows:

$$m_i \pm k \cdot u(m_x) = m_r \pm k \cdot u(m_r) + \delta m_{app} \pm k \cdot u(\delta m_{app}) + \delta m_s \pm k \cdot u(\delta m_s) + \delta m_b \pm k \cdot u(\delta m_b) , \quad (2)$$

where i denotes the nominal weight actually measured, m_r is the reference weight, δm_{app} is the approximation error, δm_s is the result of stochastic distribution in repeated measurements, and δm_b is the buoyancy effect, k is the coverage factor, and $u(x)$ is the respective standard uncertainty of each measured value. Air buoyancy is equal to the weight of the displaced air [17]:

$$F_b = V \cdot \rho_a \cdot g = \frac{m}{\rho} \cdot g , \quad (3)$$

Weights class E_2 was used, according to the International recommendation OIML R 111-1 [17]. These weights are generally intended for use in the verification or calibration of weighing instruments of special accuracy class I. Reading the resolution of the voltage signal from the strain gauge is 20 digits, which is not necessary due to measurement uncertainty and repeatability. Environmental conditions were monitored during each repetition, and respective values of temperature, humidity, and atmospheric pressure registered at the start of measurement and at its end are shown in Fig. 6.

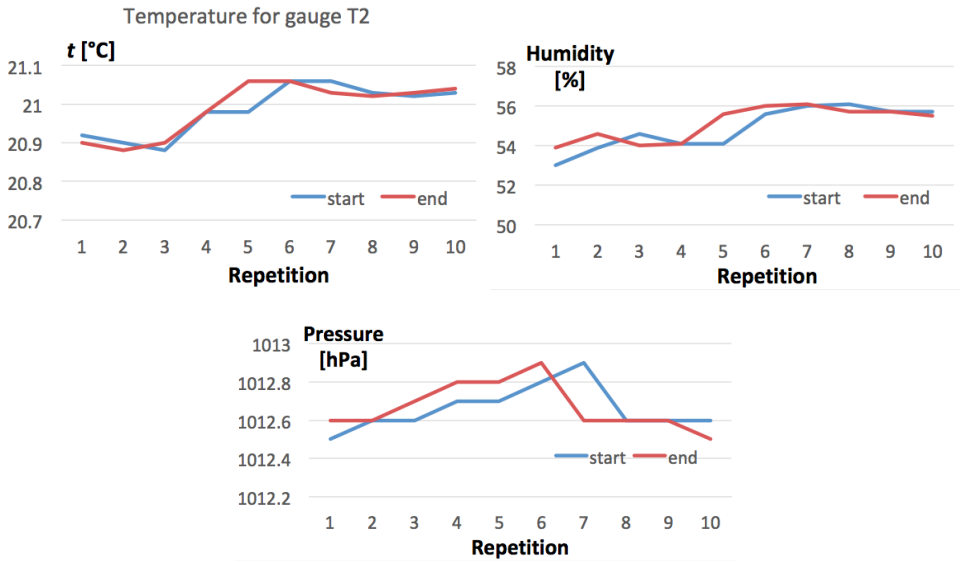

Fig. 6 Environmental conditions during calibration

Due to the very stable conditions and from a practical perspective, the buoyancy effect was found negligibly small. The maximum permissible errors (MPE) of E_2 class weights with proper certificates are collected in Table 1.

Table 1 Maximum permissible errors of the applied weights

Nominal weight	MPE
0.5 kg	±0.8 mg
1.0 kg	±1.6 mg
2.0 kg	±3.0 mg
5.0 kg	±8.0 mg
10.0 kg	±16.0 mg

Under the load, the strain gauges changed their electrical conductance, which was indicated in siemens [$S = \Omega^{-1}$]. The calibration procedure was repeated 10 times for each of three strain gauges thus enabling the statistical analysis of the obtained results. During each repetition, 100 samples were registered. Examples of histograms shown in Fig. 7 demonstrate that in each repetition, Gaussian statistics can be applied.

Based on normal distribution, Type A uncertainty [18] was calculated for each gauge, and the calibration curves were appointed. Results are presented and discussed in the next section.

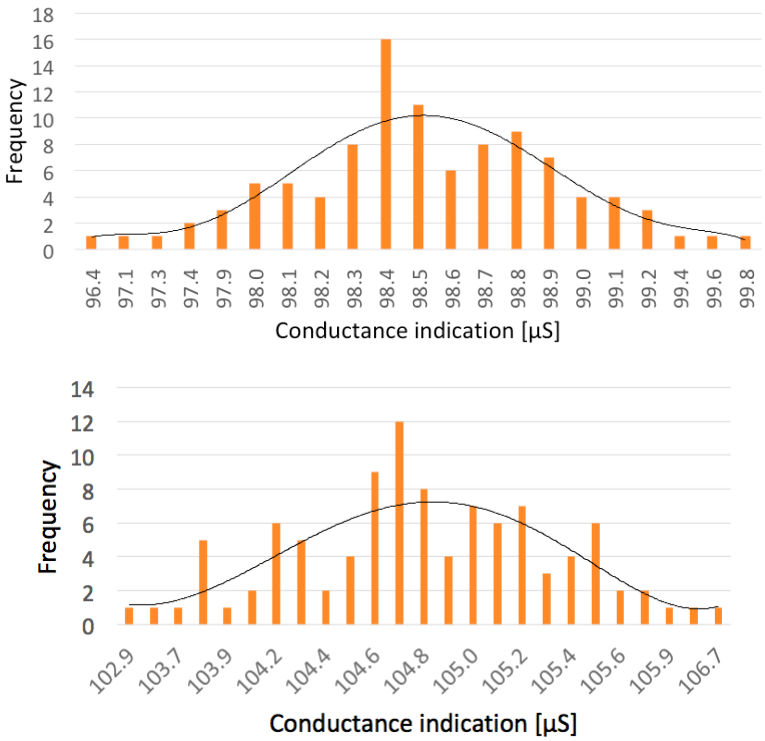

Fig. 7 Examples of the obtained histograms for two repetitions

4. Results and Discussion

Fig. 8 presents the results of 10 repetitions, each with 100 samples registered, for the strain gauge No. 1 conductance indications under a load of 0.5 kg. It was typical for every repeated procedure that the subsequent samples comprised almost straight lines, while the next repetitions provided similar lines at a different level, with different average, but with a quite similar standard deviation below 0.8, as can be seen in Table 2. Scattering of the average values from 10 repetitions appeared smaller for larger weights.

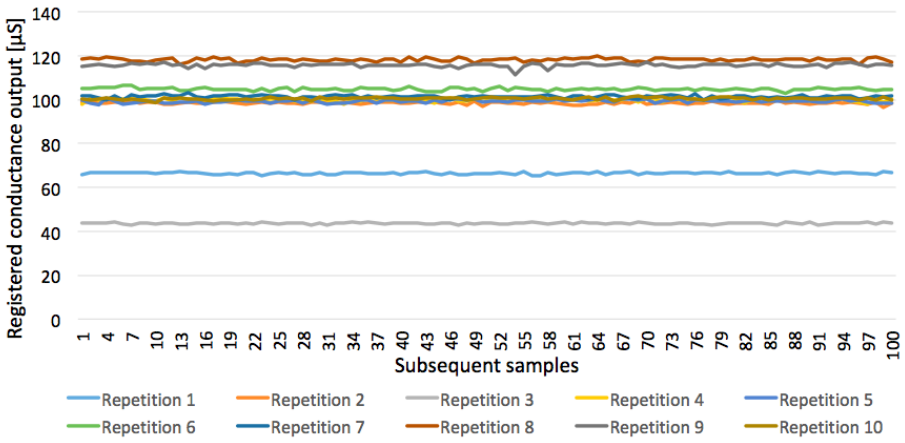

Fig. 8 Measurement results for the strain gauge No. 1 under load of 0.5 kg

Table 2 Conductance statistics for 10 repetitions, strain gauge No. 1, nominal load 0.5 kg

Repetition No.	1	2	3	4	5	6	7	8	9	10	Average $\bar{\bar{m}}_{0.5}$ [µS]
Average $\bar{m}_{0.5}$	66.5	98.5	43.6	99.9	99.3	104.8	101.4	118.3	115.7	100.5	94.9
MIN [µS]	65.2	96.4	42.7	97.9	97.7	102.9	99.8	116.1	111.2	98.6	43.6
MAX [µS]	67.5	99.8	44.2	101.5	100.7	106.7	103.0	120.0	117.3	101.8	115.7
Range R [µS]	2.2	3.4	1.5	3.6	3.0	3.8	3.2	3.8	6.1	3.1	77.3
Std.dev. s [µS]	0.471	0.510	0.332	0.677	0.598	0.624	0.653	0.738	0.794	0.568	

It can be seen that the dispersion of the results due to the stochastic distribution in repeatability conditions is several orders of magnitude higher than that of other uncertainty sources specified in Eq. (2). Thus, the Type A uncertainty based on the statistical analysis seems to be the most appropriate methodology.

It is noteworthy, however, that 10 repetitions allow for a decrease of uncertainty span, as follows [19]:

$$u(\bar{x}) = \frac{u(x)}{\sqrt{n}}, \tag{4}$$

where n is the number of repetitions, here n = 10. Thus, the standard uncertainty can be $u(\bar{\bar{m}}_{0.5})$ = 0.25 instead of $u(m_{0.5})$ = 0.794, and expanded uncertainty $U_{0.99}$ = 0.75 [µS].

Coverage factor for level of confidence 99% is assumed k = 3. Similarly, uncertainty was estimated for each measurement.

Table 3 Uncertainties for each reference weight

	$m_{r0.5}$=0.5 kg	m_{r1}=1 kg	m_{r2}=2 kg	m_{r5}=5 kg	m_{r10}=10 kg
Average $\bar{\bar{m}}_x$ [µS]	94.85	144.78	207.61	352.23	459.49
MIN [µS]	42.67	94.86	168.77	292.34	417.17
MAX[µS]	119.98	182.09	251.59	403.81	505.02
Range R [µS]	77.31	87.23	82.82	111.48	87.85
Std.dev. s_{max} [µS]	0.79	1.02	2.17	2.18	3.16
$m_x \pm U_{0.99}$ [µS]	94.85±0.75	144.78±0.97	207.61±2.05	352.23±2.07	459.49±2.99

Approximation of the obtained results led to the following conclusions. Linear function, which would be the most desirable, provided linearity error ca. 51 [µS] for the strain gauge conductance output 352 [µS], so that the approximation error was almost 15%. So it was found necessary to approximate the function with a polynomial, as follows:

$$y = -3.7x^2+77x+65. \tag{5}$$

This function provided a maximal approximation error of 7.73 [µS] for the strain gauge conductance output 94.85 [µS], so that percentage was ca. 8%. Both approximation graphs together with calibration points are shown in Fig. 9.

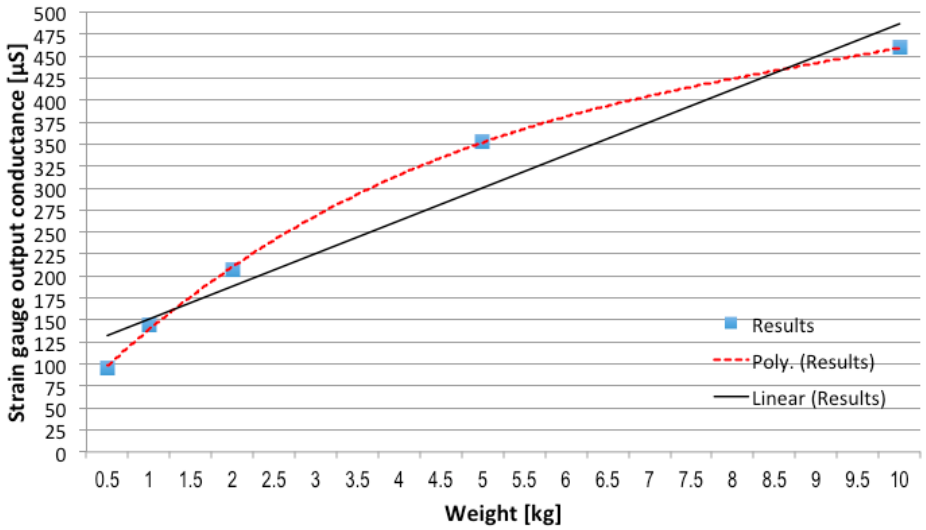

Fig. 9 Approximation functions and calibration points

The aforementioned results demonstrated that all the uncertainty components are negligibly small compared to the function approximation error. Thus, the latter can be considered the main uncertainty source for each measurement result obtained from the strain gauges during the belt tension measurement.

For practical reasons, indications in conductance units [S] should be recalculated into respective force values [N]. The formula derived from the experimental data presented above is as follows:

$$y = 136 \cdot x^{1.876}, \tag{6}$$

where x is the conductance [S], and y is the belt pressure on roller [N]. Table 4 presents the results of calibration and approximation.

Table 4 Uncertainties for each reference weight

Load [kg]	Load [N]	Conductance [μS]	Resistance [Ω]	Load indication [N]	Approximation error [N]
0.50	4.90	94.85	10542.96	4.60	0.30
1.00	9.81	144.78	6907.03	10.16	-0.35
2.00	19.61	207.61	4816.72	19.95	-0.33
5.00	49.03	352.23	2839.05	53.68	-4.65
10.00	98.07	459.49	2176.33	88.31	9.76

It is seen from Table 4 that the approximation error is below 10% of the actually measured value, which is highly satisfactory for this application aiming at the belt tension monitoring in industrial conditions.

5. CONCLUSIONS

The research studies and analysis demonstrated that the main source of uncertainty in the calibration procedure was the function of approximation, while the others were orders of magnitude smaller. Registered values revealed distribution fairly close to the expected Gaussian one, so that Type A uncertainty could be estimated from a number of measurements in repeatability conditions. Application of mean value from 10 repetitions made it possible to reduce final uncertainty even more, so that expanded uncertainty of conductance was $U_{0.99} = 0.75$ [μS], with coverage factor $k = 3$ for the level of confidence 99%. The maximal approximation error, however, was 7.73 [μS] for the strain gauge conductance output 94.85 [μS], i.e. ca. 8%. When the conductance was calculated to force values, an approximation error below 10% was obtained. This result was found very good due to the industrial application of the analyzed system.

Acknowledgements: *The authors express their gratitude to the Radwag Wagi Elektroniczne, Radom, Poland, for the possibility to perform measurements in excellent laboratory conditions*.

REFERENCES

1. Miyata, H.H., Nagano, M.S., Gupta, J.N.D., 2019, *Integrating preventive maintenance activities to the no-wait flow shop scheduling problem with dependent-sequence setup times and makespan minimization*, Computers & Industrial Engineering, 135, pp. 79-104.
2. Ruiz-Sarmiento, J.R., Monroy, J., Moreno, F.A., Galindo, C., Bpnelo, J.M., Gonzalez-Jimenez, J., 2020, *A predictive model for the maintenance of industrial machinery in the context of Industry 4.0*, Engineering Applications of Artificial Intelligence, 87, Article 103289.

3. Lin, D., Jin, B., Chang, D., 2020, *A PSO approach for the integrated maintenance model*, Reliability Engineering & System Safety, 193, Article 106625.
4. Kuboki, N., Takata, S., 2019, *Selecting the Optimum Inspection Method for Preventive Maintenance*, Procedia CIRP, 80, pp. 512-517.
5. Mörth, O., Emmanouilidis, Ch., Hafner, N., Schadler, M., 2020, *Cyber-physical systems for performance monitoring in production intralogistics*, Computers & Industrial Engineering, 142, Article 106333.
6. Gładysewicz, L., *Belt Feeders: Theory and Calculations*, Wroclaw University of Technology, Wrocław (in Polish).
7. Fedorko, G., Ivančo, V., 2012, *Analysis of Force Ratios in Conveyor Belt of Classic Belt Conveyor*, Procedia Engineering, 48, pp. 123-128.
8. Andrejiova, M., Grincova, A., Marasova, D., 2019, *Failure analysis of the rubber-textile conveyor belts using classification models*, Engineering Failure Analysis, 101, pp. 407-417.
9. Molnár, V., Fedorko, G., Homolka, L., Michalik, P., Tučková, Z., 2019, *Utilisation of measurements to predict the relationship between contact forces on the pipe conveyor idler rollers and the tension force of the conveyor belt*, Measurement, 136, pp. 735-744.
10. Mazurkiewicz, D., 2011, *Study on the chosen aspects of maintenance diagnostics of belt conveyors*, Lublin University of Technology, Lublin (in Polish).
11. Nowak, R., Grzyb, K., 2008, *Monitoring and laboratory research on the diagnostics process of feeding belts with steel rods*, Proc. 16th International Symposium "100 lat w służbie polskiego przemysłu wydobywczego", Zakopane, Poland, pp. 39-54.
12. Ryba, T., 2019, *Overview of the rubber belts tension test methods in the close transport conveyors*, Mechanik, 3, pp. 210-212.
13. Ryba, T., 2020, Patent Application No. P.432900, Warsaw, Poland.
14. Daminabo, S. C., Goel, S., Grammatikos, S. A., Nezhad, H. Y., Thakur, V. K., 2020, *Fused deposition modeling-based additive manufacturing (3D printing): techniques for polymer material systems*, Materials Today Chemistry, 16, Article 100248.
15. Tyczynski, P., Siemiatkowski, Z., Rucki, M., *Analysis of the drill base body fabricated with Additive Manufacturing technology*, Proceedings of 18th International euspen Conference & Exhibition, 4-8 June 2018, Venice, Italy, pp. 287-288
16. Kazmer, D., 2017, *Applied Plastics Engineering Handbook*, Second Edition, Elsevier, Amsterdam.
17. International Organization of Legal Metrology, 2004, OIML R 111-1: 2004, *International Recommendation: Weights of classes E_1, E_2, F_1, F_2, M_1, M_{1-2}, M_2, M_{2-3} and M_3*, Part 1: *Metrological and technical requirements*, Grande Imprimerie de Troyes, France.
18. EA-4/02 M: 2013. *Evaluation of the Uncertainty of Measurement in Calibration.*
19. JCGM 100:2008. *Evaluation of measurement data — Guide to the expression of uncertainty in measurement.*